Chemistry & Biology, Vol. 10, 503–509, June, 2003, ©2003 Elsevier Science Ltd. All rights reserved. DOI 10.1016/S1074-5521(03)00122-4

Spatiotemporal Laser Inactivation of Inositol 1,4,5-Trisphosphate Receptors Using Synthetic Small-Molecule Probes

Takanari Inoue,[1] Kazuya Kikuchi,[1,3] Kenzo Hirose,[2] Masamitsu Iino,[2] and Tetsuo Nagano[1,*]
[1]Graduate School of Pharmaceutical Sciences
[2]Department of Pharmacology
Graduate School of Medicine
The University of Tokyo
7-3-1 Hongo, Bunkyo-ku
Tokyo 113-0033
[3]PRESTO
Japan Science and Technology Corporation
Kawaguchi
Japan

Summary

A malachite green-conjugated inositol 1,4,5-trisphosphate ($MGIP_3$) induces specific inactivation of IP_3 receptor (IP_3R) in tissue samples upon laser irradiation. To verify potential usefulness of the method for studies of cellular Ca^{2+} signaling, we conducted laser inactivation at the single-cell level and show that IP_3R was inactivated with extremely high spatiotemporal resolution. In the presence of $MGIP_3$, the Ca^{2+} release function of IP_3R in single B lymphoma cells decayed exponentially with increasing duration of laser irradiation with a time constant of 3.4 s. Moreover, by confining laser irradiation to a spatially distinct region of differentiated PC12 cells, subcellular inactivation of IP_3R was attained, as revealed by a loss of local Ca^{2+} signal. Such real-time inactivation of IP_3R only within a subcellular region may provide a powerful method for investigating spatiotemporal dynamics of Ca^{2+} signaling.

Introduction

Various methods, including the use of pharmacological antagonists, targeted gene disruption, or antibodies against target molecules, have been used in specific inactivation of biomolecules to clarify their physiological functions. Recent studies emphasized the importance of the spatiotemporal aspects of signaling molecules [1–3]. Therefore, it will be extremely useful if a targeted molecule can be instantaneously inactivated at a specified time and position. Chromophore-assisted laser inactivation (CALI), originally developed by Jay, is one of the ideal methods for achieving this purpose [4]. In CALI, chromophore-labeled antibody molecules are introduced into cells, which are then subjected to laser irradiation. Upon absorption of laser energy, the chromophore mediates generation of radical species [5]. Because the radical species are highly reactive and have a very short lifetime, only the antibody-recognized proteins are specifically inactivated. By CALI, it is possible to abrogate the function of a target protein with unprecedented spatiotemporal resolution. However, CALI has several limitations that restrict wider biological applications. One of these limitations is the use of antibodies for target recognition. It is difficult to label antibody molecules with chromophores at specific amino acid residues, so the extent of the damage inflicted on the target protein cannot readily be controlled. Moreover, it is necessary to use invasive methods to introduce antibody molecules into cells, and in most CALI experiments, antibody introduction is conducted by microinjection or trituration. These methods are not universally applicable, and indeed, only a few types of cell have been studied [6].

To circumvent the above-mentioned limitation, we had previously developed a small-molecule-based CALI (smCALI), where small synthetic molecules instead of antibodies are used for molecular recognition. We used a chromophore-labeled IP_3 analog ($MGIP_3$) [7] to inactivate IP_3R by laser irradiation in small bundles of smooth muscle cells and showed that in comparison with antibody-based laser inactivation, more than 20-fold greater efficiency of receptor inactivation is realized by smCALI [8]. The efficient inactivation was reasonably explained by the proximity of the chromophore to the target molecule. The proximity was made possible by a small ligand moiety, in this case IP_3. In the present study, we applied smCALI to single cultured cells and showed that $MGIP_3$-mediated inactivation of IP_3R can be accomplished with even a lower time constant (3.4 s) than that reported in our previous study and within a subcellular region of differentiated cells. Manipulation of protein functions with such extremely high spatiotemporal resolution can be a promising method for studying complex signal pathways such as spatiotemporally regulated Ca^{2+} signals [9, 10]. Furthermore, our data suggest that smCALI requires a very low probe concentration due to rapid on and off kinetics for the binding with the target molecule, implicating a novel inactivation mechanism totally different from those of other conventional methods.

Results

Ca^{2+} Release Activity of $MGIP_3$

To measure the Ca^{2+} release activity of $MGIP_3$ (Figure 1A) within a single cell, we carried out luminal Ca^{2+} imaging using DT40 cells [11] (see Experimental Procedures for details). DT40 cells were loaded with Furaptra AM, membrane-permeant, a low-affinity Ca^{2+} indicator, which entered both the cytoplasm and organelles. Furaptra-loaded cells were then permeabilized with β-escin to remove the dye in the cytoplasm while retaining it in the endoplasmic reticulum (ER) to continuously monitor luminal Ca^{2+} concentration ($[Ca^{2+}]l$) within the Ca^{2+} store. An increase in $[Ca^{2+}]l$ was observed upon activation of sarco/endoplasmic reticulum Ca^{2+}-ATPase (SERCA) with application of both Ca^{2+} and MgATP, followed by a decrease upon IP_3 addition (Figure 1B). This Ca^{2+} loading and release procedure can be repeated in the same cells. The Ca^{2+} release activity of test compounds was

*Correspondence: tlong@mol.f.u-tokyo.ac.jp

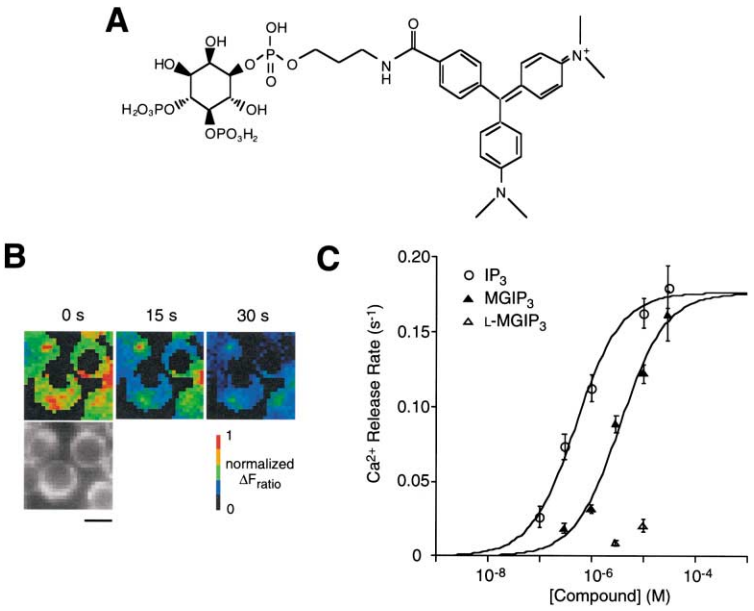

Figure 1. Ca^{2+} Release Activity of $MGIP_3$ in DT40 Cells

(A) Structure of $MGIP_3$.

(B) Fluorescence images of wild-type DT40 cells excited at 380 nm after loading Furaptra AM and subsequent permeabilization, and pseudocolor images of the cells during Ca^{2+} release upon addition of IP_3. Scale bar, 10 μm.

(C) $MGIP_3$ and its analogs induced Ca^{2+} release via IP_3R expressed in wild-type DT40 cells. The average initial rates of Ca^{2+} release are plotted against test compound concentrations (IP_3, circles, $n \geq 7$; $MGIP_3$, closed triangles, $n \geq 11$; L-$MGIP_3$, open triangles, $n \geq 6$). Error bars represent SEM.

estimated by fitting an exponential function to the initial part of the time course of IP_3-induced Ca^{2+} release (IICR). Both IP_3 and $MGIP_3$ induced Ca^{2+} release in a dose-dependent manner with EC_{50} values of 0.5 μM and 3.6 μM, respectively, at 300 nM Ca^{2+} (Figure 1C). An optical isomer of $MGIP_3$, L-$MGIP_3$, had almost no Ca^{2+} release activity even at concentrations as high as 10 μM, confirming that IP_3R stereospecifically recognizes these ligands [12].

Laser Inactivation of IP_3R

We investigated whether a laser beam focused onto single DT40 cells in the presence of $MGIP_3$ induces protein inactivation. First, by monitoring $[Ca^{2+}]I$ within permeabilized DT40 cells, we measured the IICR rate at 10 μM IP_3. The cells were then irradiated for 15 s in the presence of 3 μM $MGIP_3$. After wash-out of $MGIP_3$, the IICR rate was measured again and compared with that at pretreatment. A considerable decrease in the IICR rate was observed (IICR rate pretreatment = 0.101 ± 0.010 s^{-1}, IICR rate posttreatment = 0.046 ± 0.008 s^{-1}; Figures 2A and 2B). The inactivation was irreversible for at least 10 min since there was no recovery of the IICR rate measured 10 min after irradiation (data not shown). On the other hand, laser irradiation alone in the absence of $MGIP_3$ had no effect on the IICR rate (Figure 2B). The $MGIP_3$-mediated laser inactivation was dependent on $MGIP_3$ concentration, as revealed by the experiment in which various $MGIP_3$ concentrations were added to the cells subjected to 5 s laser irradiation (IC_{50} = 1.9 μM; Figure 2C).

We then studied if laser-induced inactivation of IP_3R also occurs in the presence of L-$MGIP_3$, instead of $MGIP_3$. L-$MGIP_3$ can be an ideal negative control because it has a photochemical nature similar to that of $MGIP_3$, except for its slight activity against IP_3R, as shown in Figure 1. When laser irradiation was carried out for 15 s in the presence of 3 μM L-$MGIP_3$, no effect on IP_3R activity was observed (Figure 2B), indicating no artificial laser damage on IP_3R induced by unbound malachite green. Moreover, 3 μM $MGIP_3$-mediated inactivation was greatly suppressed (Figure 2B) when the experiment was carried out in the presence of 10 μM IP_3, which competes for the binding site of IP_3R. These results indicate that $MGIP_3$-mediated inactivation of IP_3R occurs only when the probe is allowed to bind to IP_3R.

We investigated the target specificity of $MGIP_3$-mediated inactivation. SERCA proteins are colocalized with IP_3R on the same ER membrane [13] and transport Ca^{2+} into Ca^{2+} stores [14]. We compared the rate of Ca^{2+} loading, as an indicator of SERCA activity, before and after 15 s laser irradiation. There was no significant effect of laser irradiation in the absence or presence of 3 μM $MGIP_3$ (relative IICR rate = 100% ± 4% or 93% ± 3%, respectively; p = 0.23). This result suggests that no nonspecific damage to nontargeted proteins present on the same intracellular organelle with IP_3R was induced by laser irradiation.

Spatial and Temporal Resolution of smCALI

To determine whether $MGIP_3$-mediated inactivation of IP_3R is spatially controlled by laser irradiation, we compared the Ca^{2+} release activities of two adjacent cells with or without irradiation (Figure 3A). The cells exposed to 3 μM $MGIP_3$ and 15 s laser irradiation showed a considerable decrease in IP_3R activity (Figure 3Ba and Figure 3C, filled column). On the other hand, there was no change in IICR rate in nonirradiated cells immediately adjacent to the irradiated cells (Figure 3Bb and Figure 3C, open column). Thus, the region of IP_3R inactivation can be spatially controlled by laser irradiation.

To evaluate the time course of $MGIP_3$-mediated laser inactivation of IP_3R, we carried out experiments in which irradiation duration was varied. The inactivation induced by 10 μM $MGIP_3$ occurred exponentially with a time constant of 3.4 s (Figure 3D).

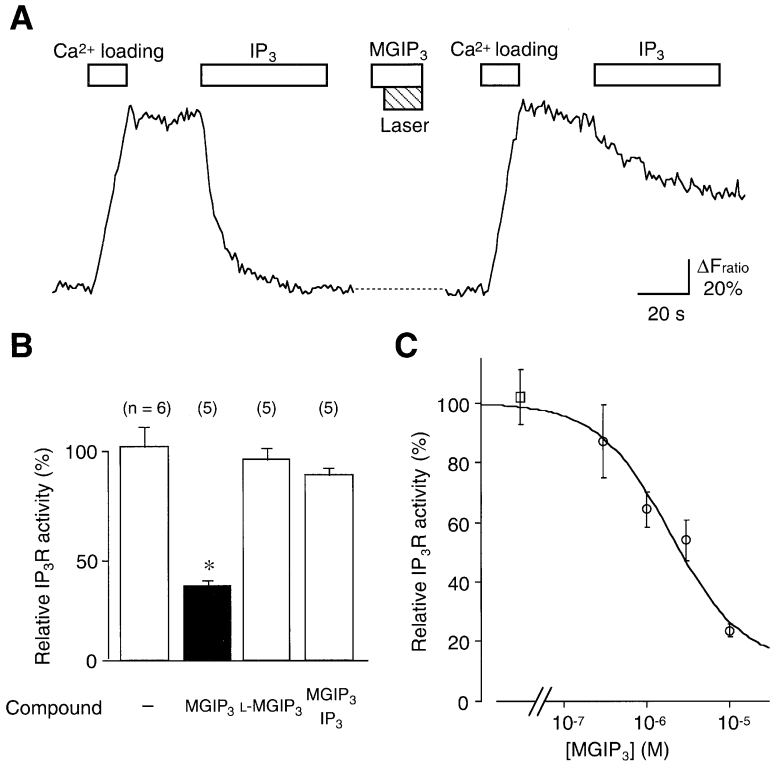

Figure 2. $MGIP_3$-Mediated Laser Inactivation of IP_3R

(A) After measurement of the IICR rate at 10 μM IP_3, permeabilized wild-type DT40 cells were pretreated with 3 μM $MGIP_3$, followed by laser irradiation for 15 s. After the irradiation and the immediate washout of $MGIP_3$-containing solution, the IICR rate at 10 μM IP_3 of the irradiated cells was measured. Note that a considerable difference in the IICR rate before and after the treatment was observed.

(B) The IICR rate after 15 s laser irradiation with or without the test compounds was normalized to that before irradiation. The compounds used were 3 μM $MGIP_3$, 3 μM L-$MGIP_3$, and 3 μM $MGIP_3$ with 10 μM IP_3. Significant difference was found only when the relative Ca^{2+} release rate of the $MGIP_3$-treated cells (closed column) was compared with those of cells under other conditions (*$p < 0.0001$, Fisher's PLSD test). The number of experiments is indicated on top of each column. Error bars represent SEM.

(C) Various concentrations of $MGIP_3$ were applied to permeabilized wild-type DT40 cells, followed by laser irradiation for 5 s, and the relative IICR rates were plotted against the $MGIP_3$ concentration (circles). The plots were fitted by a bimolecular interaction model. A relative IICR rate in the absence of $MGIP_3$ is indicated by a square. Error bars represent SEM; $n \geq 3$.

IP_3R Subtypes and smCALI

There are three subtypes of IP_3R (IP_3R-1, IP_3R-2, and IP_3R-3) that may form heterotetramers [15, 16] whose compositions may vary depending on cell type and developmental stage [17–19]. To determine whether $MGIP_3$-mediated laser inactivation affects all IP_3R subtypes, we carried out experiments using mutant DT40 cells genetically engineered to express only one of the three IP_3R subtypes, instead of wild-type cells that express all subtypes [11, 20]. In the presence of 1 μM $MGIP_3$, 15 s laser irradiation reduced IP_3R activity in all mutant cells (Figure 4A). This result shows that ligand-

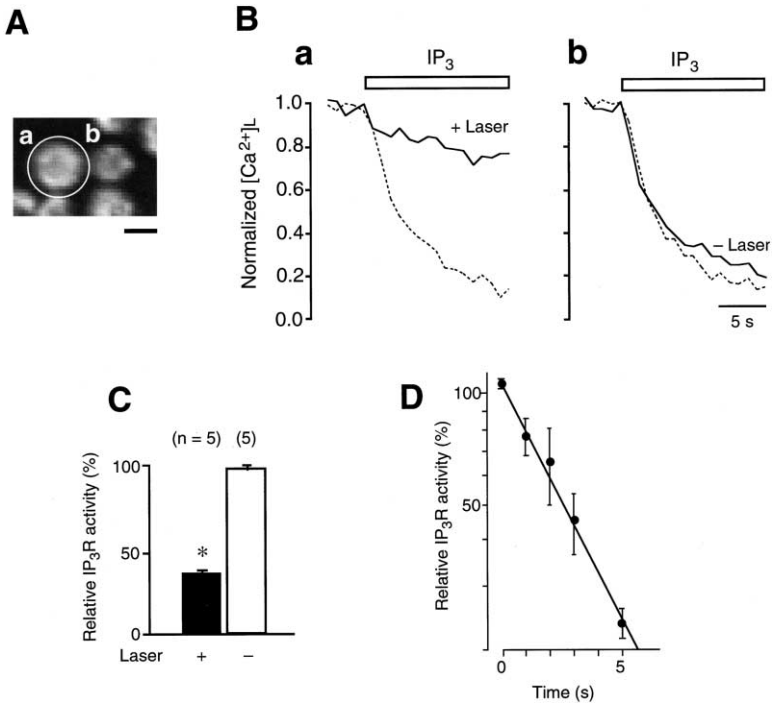

Figure 3. Spatiotemporally Controlled Inactivation of IP_3R

(A) Fluorescence image of wild-type DT40 cells excited at 380 nm after loading Furaptra AM and subsequent permeabilization. The white circle indicates the laser spot for irradiation. Scale bar, 10 μm.

(B) Time courses of IICR before and after the treatment. Luminal Ca^{2+} concentration ($[Ca^{2+}]_l$) was monitored. Application of 10 μM IP_3 is indicated by the horizontal bars. After measurement of IICR rate (dotted traces), one of the cells, (Aa), was irradiated for 15 s in the presence of 3 μM $MGIP_3$. Then, the IICR rate was measured again (continuous traces), resulting in a considerable reduction of IP_3R activity (Ba), while no effect was observed in the nonirradiated cell (Ab and Bb).

(C) Relative IP_3R activities of irradiated cells (closed column) and nonirradiated cells (open column). *$p < 0.0001$.

(D) Wild-type DT40 cells were subjected to irradiation for various durations in the presence of 10 μM $MGIP_3$. The ratio of the Ca^{2+} release rate after the treatment to that before the treatment is semi-log plotted ($n \geq 3$). The time constant for inactivation was calculated to be 3.4 s from an exponential fitting of these plots. Error bars represent SEM.

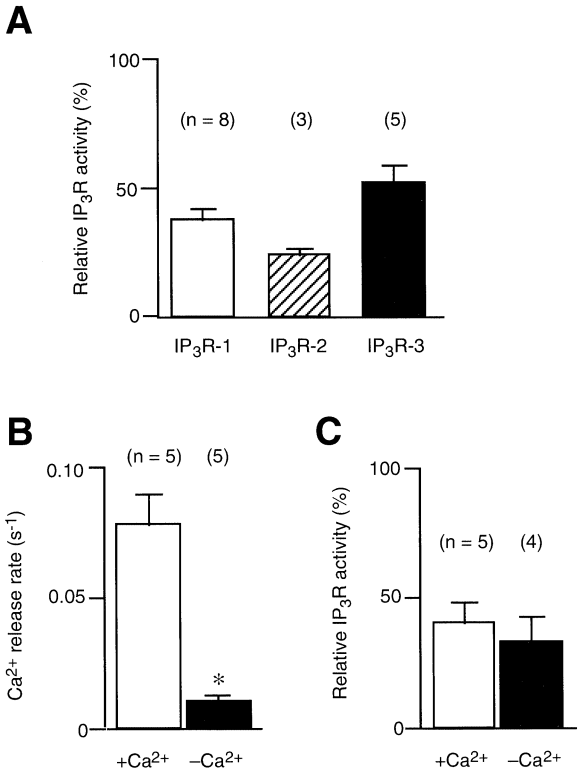

Figure 4. Characterization of $MGIP_3$-Mediated Laser Inactivation

(A) The IICR rates before and after laser inactivation were measured using mutant DT40 cells expressing only one of the three IP_3R subtypes. During irradiation, cells were treated with 1 μM $MGIP_3$ and subjected to 15 s laser irradiation. Relative Ca^{2+} release rates of cells expressing IP_3R-1 ($n \geq 4$, open column), IP_3R-2 ($n \geq 3$, hatched column), and IP_3R-3 ($n \geq 7$, closed column) are shown.

(B) 1 μM $MGIP_3$-induced Ca^{2+} release rates of IP_3R-2-expressing DT40 cells either with (open column) or without (closed column) 300 nM Ca^{2+} are shown. *$p < 0.001$.

(C) IICR rates before and after laser inactivation were measured using IP_3R-2-expressing DT40 cells. During 10 s laser irradiation, cells were treated with 1 μM $MGIP_3$ in the presence or absence of 300 nM Ca^{2+}. The relative IICR rates of the Ca^{2+}-treated cells ($n \geq 8$, open column) and Ca^{2+}-untreated cells ($n \geq 9$, closed column) are shown; $p = 0.67$. Error bars represent SEM.

modified probes such as $MGIP_3$ can simultaneously inactivate all IP_3R subtypes.

Inactivation Independent of IP_3R Channel Gating

We investigated whether $MGIP_3$-induced laser inactivation depends on IP_3R channel gating. We carried out laser irradiation in the presence of $MGIP_3$-containing solution with or without Ca^{2+}, because IP_3R channel opening is modulated by cytoplasmic Ca^{2+} concentration ($[Ca^{2+}]c$) [11, 21, 22]. Before performing the experiments on laser irradiation, whether $MGIP_3$-induced IP_3R channel opening depends on $[Ca^{2+}]c$ was also tested. We measured the 1 μM $MGIP_3$-induced Ca^{2+} release rate in the presence or absence of 300 nM Ca^{2+} using permeabilized DT40 cells expressing IP_3R-2. A significant difference in Ca^{2+} release rate between treatments with or without Ca^{2+} ($p < 0.001$; Figure 4B) was observed. We then carried out 10 s laser irradiation in the presence of 1 μM $MGIP_3$ with or without 300 nM Ca^{2+}, and compared IICR rates before and after these treatments. Regardless of the presence of Ca^{2+}, comparable inactivation of IP_3R occurred under both conditions ($p = 0.67$; Figure 4C). These results indicate that $MGIP_3$-induced laser inactivation occurs independently of the IP_3R channel gating.

Inactivation of IP_3Rs in a Subcellular Region

To determine whether laser inactivation of IP_3R is achieved at the subcellular level, we applied the present method to differentiated PC12 cells. After treatment with a nerve growth factor (NGF), PC12 cells differentiated to form varicosities separated by a long neurite from a soma (Figure 5A). A laser beam was aligned to focus onto the varicosites. After a control solution or $MGIP_3$-containing solution was applied to the cells via glass pipettes in the whole-cell configuration, the varicosities were either nonirradiated or irradiated for 30 s. The cells were then stimulated with 100 nM bradykinin (BK) in a Ca^{2+}-free medium. BK stimulation activates phospholipase C, subsequent IP_3 production, and IP_3Rs [23, 24]. We estimated IP_3R activity from the Ca^{2+} flux rate in response to BK [25]. When we used a control internal solution, subsequent 30 s irradiation of the varicosities did not alter IP_3R activity when compared with that of nonirradiated cells, revealing that no laser damage was induced (flux rate nonirradiated $= 0.131 \pm 0.082\ s^{-1}$, flux rate irradiated $= 0.143 \pm 0.043\ s^{-1}$; $p = 0.5224$; data not shown). When we used an internal solution containing 10 μM $MGIP_3$, neither $[Ca^{2+}]c$ increase during the whole-cell application nor significant attenuation of BK responses in the absence or presence of 10 μM $MGIP_3$ ($0.131 \pm 0.082\ s^{-1}$ and $0.133 \pm 0.052\ s^{-1}$, respectively; $p = 0.2689$) was observed. When we applied 30 μM or higher concentration of $MGIP_3$, we detected Ca^{2+} increase in the cytoplasm and subsequent diminished response to BK (data not shown). On the contrary, subsequent 30 s irradiation of the varicosities of 10 μM $MGIP_3$-applied cells caused a considerably small BK response that reflects extensive decrease in the IP_3R activity of the region ($p < 0.05$; Figures 5B and 5C). Even under these conditions, the IP_3R activity of the soma within the same cell did not change significantly ($p = 0.3855$; Figures 5B and 5C). These results clearly demonstrate that $MGIP_3$-mediated laser inactivation of IP_3R could be carried out within a subcellular region of a single nonpermeabilized cell.

Discussion

We demonstrated that spatiotemporally controlled inactivation of a target protein function can be induced using a small-molecule probe and a laser beam. We have already shown that small-molecule-based laser inactivation is more than 20 times more efficient than antibody-based CALI, which may be due to the spatial proximity of the chromophore to the target protein [8]. Here we showed that the small-molecule probe could induce extensive protein inactivation within a few seconds ($t_{1/2} = 2.6$ s; Figure 3D), which was even more rapid than our previously reported results ($t_{1/2} = 4$ min) [8]. Considering an

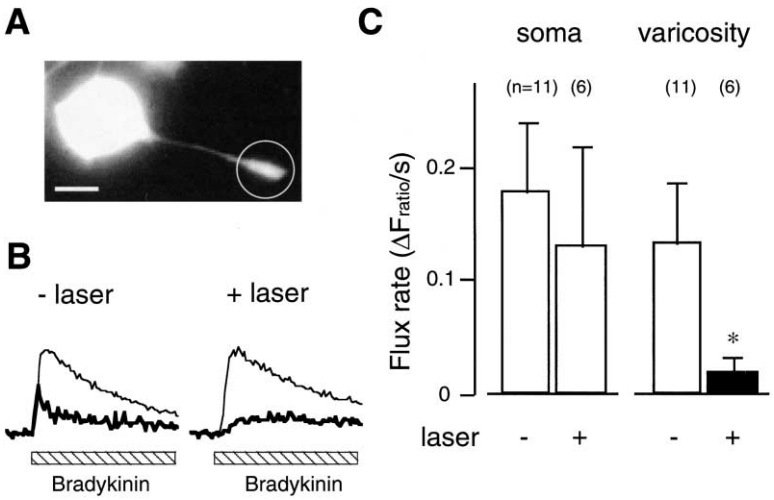

Figure 5. IP_3R Inactivation at a Varicosity by Subcelluar Laser Irradiation

(A) Fluorescence image of differentiated PC12 cells loaded with Fura2. The white circle presented onto a varicosity indicates the laser spot for irradiation. Scale bar, 10 μm.

(B) After whole-cell application of 10 μM $MGIP_3$-containing solution, cells were either nonirradiated or irradiated for 30 s. After the treatment, cells were stimulated with BK, and the obtained responses within a soma (thin traces) and a varicosity (thick traces) were superimposed, with respective conditions noted above each trace.

(C) The flux rate of Ca^{2+} in response to BK was presented under respective conditions. Flux rate reflects IP_3R activity and was calculated from the slope of BK response shown in (B). Significant difference was found when, in the presence of $MGIP_3$, the flux rate of irradiated cells and that of nonirradiated cells were compared; *$p < 0.05$. The number of experiments is indicated on top of each column. Error bars represent SEM.

irradiation period longer than 5 min is normally required for antibody-based CALI [6], the inactivation time constant obtained in this study is extremely short. Furthermore, the area of inactivation can be precisely controlled by focusing a laser beam at the single-cell level (Figure 3C) or the subcellular level (Figure 5). Spatiotemporally controlled inactivation was attained within not only permeabilized cells but also nonpermeabilized cells, which indicates the broader applicability of smCALI over other conventional methods. Therefore, the present method may provide us with new opportunities to study rapid biological processes and subcellular behavior of signaling molecules. Such spatiotemporal regulation is important for understanding of complicated signal transduction pathways and is technically difficult to study by other conventional methods involving slower inactivation, such as the use of knockouts or RNAi. We also demonstrated that ligand-modified probes can simultaneously inactivate all IP_3R subtypes (Figure 4A). This result indicates that the use of ligand-modified probes is advantageous compared to that of antibody probes in that we need not prepare all chromophore-conjugated antibodies for the respective subtypes of respective species, which is extremely laborious. As for the ligand, only one probe is sufficient for simultaneous inactivation of all protein subtypes, because ligand recognition of its receptor is generally conserved between subtypes and species (for review, see [9, 26] for IP_3R). While antibody probes are useful in the analysis of respective subtypes, in such a case that disruption of a certain subtype by an antibody probe leads to nonexhibition of a phenotype due to compensation by other redundant subtypes, inactivation of all subtypes using smCALI is useful.

$MGIP_3$ may behave similarly to a catalytic enzyme; i.e., $MGIP_3$ exerts an irreversible effect on its substrates (IP_3Rs) with the help of a cofactor (laser energy), while $MGIP_3$ does not change during this process. Indeed, $MGIP_3$-mediated protein inactivation has enzymatic-reaction-like features, e.g., irreversible target inactivation, fast association with and fast dissociation from its target [7], and repetitive excitation of malachite green [4]. Due to cumulative inactivation of IP_3R by $MGIP_3$, even a low $MGIP_3$ concentration may eventually inactivate all IP_3Rs given a sufficiently long duration of laser irradiation. Our data are consistent with this notion, where we showed that IP_3R-3, the subtype known to have low affinity for IP_3, is effectively inactivated by 1 μM $MGIP_3$ (Figure 4A), which scarcely induces Ca^{2+} release (release rate = 0.001 s^{-1}; data not shown). Such a mode of protein inactivation is unique to small-molecule-based laser inactivation. For example, classical antagonists exhibit an inhibitory effect only at the moment of their target binding, and this effect does not persist once the antagonists dissociate from their target. Antibody-based probes used in conventional CALI bind and inactivate their target proteins under laser irradiation. However, this process may not be repeatable, because antibody probes do not usually bind repetitively to their target molecules due to their very low dissociation rate from antigens. Therefore, sufficient inhibition cannot be attained unless the concentration of antagonists greatly exceeds its K_d value or the molar ratio between the antibody probe and the antigen is greater than unity.

One may think that an agonistic effect of $MGIP_3$ on IP_3R, as shown in Figure 1, may be a problem, which may in turn exert some artificial effects before IP_3R inactivation. However, considering the cumulative nature of the smCALI mentioned above, we may be able to determine an appropriate concentration of $MGIP_3$ which does not induce detectable $[Ca^{2+}]c$ increase but is still sufficient to induce significant IP_3R inactivation. Indeed, this was observed in varicosities of differentiated PC12 cells, because we observed neither a $[Ca^{2+}]c$ increase during whole-cell application of 10 μM $MGIP_3$ nor a significant attenuation of BK responses in the absence or presence of 10 μM $MGIP_3$. However, varicosity-targeted laser irradiation in the presence of 10 μM $MGIP_3$ caused a significant decrease in BK responses (Figure 5). Thus, while an agonist effect appears to be an inherent drawback

of smCALI whereby a ligand is used for target recognition, this could be compensated by the proposed characteristic mechanism of smCALI.

Significance

Some variations of CALI other than smCALI have been developed. For example, genetically encoded target proteins fused to GFP can be inactivated by GFP excitation (GFP-CALI) [27]. Arsenic chromophore derivatives designed to specifically bind to a tetracysteine tag attached to a target protein induce target inactivation under light illumination (FlAsH-FALI) [28]. The transcripts of a target gene incorporating a chromophore binding RNA motif can be cleaved by laser irradiation, which may disrupt transcription [29]. Although these methods are powerful for cell biological studies, they inactivate genetically manipulated or overexpressed exogenous transcripts or proteins. On the contrary, completely endogenous proteins are targeted and inactivated by smCALI. In the present study, we clearly demonstrated that chromophore-conjugated ligands such as $MGIP_3$ could be used as very efficient probes for spatiotemporal inactivation of the target protein, IP_3R. The spatiotemporal dynamics of Ca^{2+} has been presumed to be an important factor for regulation of various signal transductions [9, 10]. Since IP_3R is one of the most important molecules regulating changes in $[Ca^{2+}]c$, spatiotemporal inactivation of IP_3R using $MGIP_3$ and a laser beam may provide a useful method for elucidating the complex Ca^{2+} signaling mechanism.

Experimental Procedures

Cell Culture

DT40 chicken B lymphoma cells were cultured in RPMI1640 supplemented with 10% fetal calf serum, 1% chicken serum, penicillin (100 U/ml), streptomycin (100 U/ml), and 2 mM glutamine. Various types of DT40 cell genetically manipulated to express only one of the three IP_3R subtypes were prepared as previously reported [8–10]. PC12 cells highly sensitive to NGF were purchased from Health Science Research Resources Bank (PC12 HS, JCRB0262). PC12 cells were cultured in DMEM supplemented with 10% horse serum, 5% fetal calf serum, penicillin (100 U/ml), streptomycin (100 U/ml), and 2 mM glutamine.

Luminal Ca^{2+} Imaging of DT40 Cells

Ca^{2+} imaging was performed as described previously [8]. Briefly, DT40 cells were fixed on glass coverslips double-coated with poly-L-lysine (Sigma) and collagen (IFP) in advance. After loading the cells with 20 μM Furaptra AM (Molecular Probes) for 60 min in a physiological salt solution (PSS; 150 mM NaCl, 4 mM KCl, 1 mM $MgCl_2$, 2 mM $CaCl_2$, 5.6 mM glucose, and 5 mM HEPES [pH 7.4]) containing 0.1% bovine serum albumin (BSA), they were permeabilized by incubation with 60 μM β-escin (Sigma) for 2–4 min to wash out Furaptra in the cytoplasm, which enabled measurement of Ca^{2+} concentration within the organelles ($[Ca^{2+}]l$). An inverted microscope (IX70, Olympus), equipped with a cooled CCD camera (Photometrics) and a polychromatic illumination system (T.I.L.L. Photonics), was used to capture the fluorescence images by alternate excitations at 350 and 380 nm per second. The solution around cells was sequentially changed using an electrically controlled puffing pipette to load and release Ca^{2+} from the Ca^{2+} stores of the cells. Solutions containing various concentrations of Ca^{2+} were prepared by mixing CaEGTA and EGTA solutions at an appropriate ratio [11]. The slope of the time course of the increase in $[Ca^{2+}]l$ induced by the addition of $Mg\text{-}ATP^{2-}$ in the presence of 400 nM Ca^{2+} was used as an indicator of the pump activity of sarco/endoplasmic reticulum Ca^{2+}-ATPase (SERCA). After Ca^{2+} loading, IP_3 or other test compounds in the presence or absence of 300 nM Ca^{2+} were applied to evoke Ca^{2+} release from the Ca^{2+} stores. The initial part of the normalized time course of the decrease in $[Ca^{2+}]l$ was fitted by a single exponential function, e^{-rt}, where r is the rate constant used as an index of IP_3R activity.

Cytoplasmic Ca^{2+} Imaging of PC12 Cells

To induce differentiation, 50 ng/ml 7S nerve growth factor (NGF, Invitrogen) in complete culture medium with a serum level reduced to one-eighth was applied to PC12 cells fixed on a poly-L-lysine-coated glass-bottom dish (MatTek). The NGF-containing medium was changed every other day. Cells cultured 4–7 days after initial NGF application were used for the CALI experiments. For cytoplasmic Ca^{2+} ($[Ca^{2+}]c$) imaging, cells were loaded with 5 μM Fura2 AM (Molecular Probes) in PSS containing 0.1% BSA for ~40 min. Fluorescence images were captured using the same system and protocol as those used for $[Ca^{2+}]l$ imaging. For quantification of IP_3R activity, we calculated the slope of the time course of the increase in $[Ca^{2+}]c$ induced by the addition of 100 nM bradykinin (BK, sigma) in Ca^{2+}-free PSS with 5 mM EGTA. This parameter indicates the open probability of IP_3Rs during the main activation phase in hepatocytes and neurons [23].

Laser Irradiation for $MGIP_3$ Excitation

A nitrogen-driven pulsed dye laser (wavelength 635 nm, pulse width 3 ns, and pulse energy ~30 μJ at 20 Hz; Laser Science Inc., VSL-337ND-S and DUO-220) was spatially filtered using a pair of objective lenses. A circular beam with the required spot size was introduced into an oil-immersion objective (100×, NA 1.35, Olympus) attached to an inverted fluorescence microscope. The laser beam was focused onto single DT40 cells. The diameters of the laser spot and the single DT40 cells were 20 μm and ~15 μm, respectively. The laser pulse energy at the focal plane was 11–14 μJ. Laser irradiation was carried out as follows: After measurement of the IP_3-induced Ca^{2+} release (IICR) rate at 10 μM IP_3, permeabilized DT40 cells were pretreated with or without the respective test compounds for 5 s and then irradiated. After the irradiation, the test-compound-containing solution around the cells was immediately washed out with a solution containing 10 mM EGTA. The IICR rate at 10 μM IP_3 of the irradiated cell was then measured again and compared to that before the treatment. As for the analysis of nonirradiated cells surrounding irradiated cells, we randomly selected cells within 20 μm away from the irradiated cells.

For subcellular irradiation, a laser beam was focused onto the varicosities of differentiated PC12 cells. Each varicosity was separated from a soma by a long neurite (48 ± 11 μm, mean ± SD, n = 35). The diameter of the laser spot was 15 μm, and a single varicosity was well covered by the spot. The laser pulse energy at the focal plane was 6 μJ. Somatic whole-cell applications were carried out using patch pipettes pulled from 1.5 mm diameter glass capillaries (Harvard Clark). The pipette internal solution contained 140 mM potassium-gluconate, 4 mM NaCl, 4 mM Mg-ATP, 0.3 mM Na-GTP, 0.1 mM Fura2, and 10 mM HEPES (pH adjusted to 7.4 with KOH). In some experiments, the test compounds were added to the internal solution. Resistances of pipettes were ~2–5 MΩ when filled with an internal solution. Subcellular irradiation was carried out 5 min after membrane rupture, at which time small molecules in the pipettes were well diffused into the cells, as estimated by the fluorescence signal of Fura2. After the irradiation, 100 nM BK in the Ca^{2+}-free PSS containing 5 mM EGTA was extracellularly applied, and the $[Ca^{2+}]c$ signal obtained from a varicosity and that from a soma was compared. Membrane potential was clamped at −70mV during measurements. All experiments were carried out at room temperature (24°C).

Statistical Analyses

Statistical analysis was performed using an unpaired t test or Fisher's PLSD test for DT40 experiments and a nonparametric Mann-Whitney test for PC12 experiments.

Acknowledgments

This study was supported in part by the Ministry of Education, Culture, Sports, Science and Technology of Japan (Advanced and Innovational Research Program in Life Sciences and grants 13024217, 13558078, 1367232, and 14045210 to K.K.), Takeda Science Foundation, Nagase Science and Technology Foundation, and Sankyo Foundation. T.I. is a recipient of a fellowship for young scientists from the Japanese Society for the Promotion of Science.

Received: February 10, 2003
Revised: April 4, 2003
Accepted: April 22, 2003
Published: June 20, 2003

References

1. Schmucker, D., Su, A.L., Beermann, A., Jäckle, H., and Jay, D.G. (1994). Chromophore-assisted laser inactivation of patched protein switches cell fate in the larval visual system of *Drosophila*. Proc. Natl. Acad. Sci. USA *91*, 2664–2668.
2. Vernos, I., Raats, J., Hirano, T., Heasman, J., Karsenti, E., and Wylie, C. (1995). Xklp1, a chromosomal *Xenopus* kinesin-like protein essential for spindle organization and chromosome positioning. Cell *81*, 117–127.
3. Kiselyov, K., Xu, X., Mozhayeva, G., Kuo, T., Pessah, I., Mignery, G., Zhu, X., Birnbaumer, L., and Muallem, S. (1998). Functional interaction between $InsP_3$ receptors and store-operated Htrp3 channels. Nature *396*, 478–482.
4. Jay, D.G. (1988). Selective destruction of protein function by chromophore-assisted laser inactivation. Proc. Natl. Acad. Sci. USA *85*, 5454–5458.
5. Liao, J.C., Roider, J., and Jay, D.G. (1994). Chromophore-assisted laser inactivation of proteins is mediated by the photogeneration of free radicals. Proc. Natl. Acad. Sci. USA *91*, 2659–2663.
6. Jay, D.G., and Sakurai, T. (1999). Chromophore-assisted laser inactivation (CALI) to elucidate cellular mechanisms of cancer. Biochim. Biophys. Acta *1424*, M39–M48.
7. Inoue, T., Kikuchi, K., Hirose, K., Iino, M., and Nagano, T. (1999). Synthesis and evaluation of 1-position-modified inositol 1,4,5-trisphosphate analogs. Bioorg. Med. Chem. Lett. *9*, 1697–1702.
8. Inoue, T., Kikuchi, K., Hirose, K., Iino, M., and Nagano, T. (2001). Small molecule-based laser inactivation of inositol 1,4,5-trisphosphate receptor. Chem. Biol. *8*, 9–15.
9. Ernesto, C., and Claude, K. (1999). Calcium as a Cellular Regulator (New York: Oxford University Press).
10. Berridge, M.J., Lipp, P., and Bootman, M.D. (2000). The versatility and universality of calcium signalling. Nat. Rev. Mol. Cell Biol. *1*, 11–21.
11. Miyakawa, T., Maeda, A., Yamazawa, T., Hirose, K., Kurosaki, T., and Iino, M. (1999). Encoding of Ca^{2+} signals by differential expression of IP_3 receptor subtypes. EMBO J. *18*, 1303–1308.
12. Strupish, J., Cooke, A.M., Potter, B.V.L., Gigg, R., and Nahorski, S.R. (1988). Stereospecific mobilization of intracellular Ca^{2+} by inositol 1,4,5-trisphosphate. Biochem. J. *253*, 901–905.
13. Hirose, K., and Iino, M. (1994). Heterogeneity of channel density in inositol-1,4,5-trisphosphate-sensitive Ca^{2+} stores. Nature (Lond.) *372*, 791–794.
14. Thastrup, O., Cullen, P.J., Drøbak, B.K., Hanley, M.R., and Dawson, A.P. (1990). Thapsigargin, a tumor promoter discharges intracellular Ca^{2+} stores by specific inhibition of the endoplasmic reticulum Ca^{2+}-ATPase. Proc. Natl. Acad. Sci. USA *87*, 2466–2470.
15. Joseph, S.K., Lin, C., Pierson, S., Thomas, A.P., and Maranto, A.R. (1995). Heteroligomers of type-I and type-III inositol trisphosphate receptors in WB rat liver epithelial cells. J. Biol. Chem. *270*, 23310–23316.
16. Monkawa, T., Miyawaki, A., Sugiyama, T., Yoneshima, H., Yamamoto-Hino, M., Furuichi, T., Saruta, T., Hasegawa, M., and Mikoshiba, K. (1995). Heterotetrameric complex formation of inositol 1,4,5-trisphosphate receptor subunits. J. Biol. Chem. *270*, 14700–14704.
17. Newton, C.L., Mignery, G.A., and Südhof, T.C. (1994). Co-expression in vertebrate tissues and cell lines of multiple inositol 1,4,5-trisphosphate ($InsP_3$) receptors with distinct affinities for $InsP_3$. J. Biol. Chem. *269*, 28613–28619.
18. Wojcikiewicz, R.J. (1995). Type I, II and III inositol 1,4,5-trisphosphate receptors are unequally susceptible to down-regulation and are expressed in markedly different proportions in different cell types. J. Biol. Chem. *270*, 11678–11683.
19. Dent, M.A., Raisman, G., and Lai, F.A. (1996). Expression of type 1 inositol 1,4,5-trisphosphate receptor during axogenesis and synaptic contact in the central and peripheral nervous system of developing rat. Development *122*, 1029–1039.
20. Sugawara, H., Kurosaki, M., Takata, M., and Kurosaki, T. (1997). Genetic evidence for involvement of type 1, type 2 and type 3 inositol 1,4,5-trisphosphate receptors in signal transduction through the B-cell antigen receptor. EMBO J. *16*, 3078–3088.
21. Iino, M. (1990). Biphasic Ca^{2+} dependence of inositol 1,4,5-trisphosphate-induced Ca^{2+} release in smooth muscle cells of the guinea pig taenia caeci. J. Gen. Physiol. *95*, 1103–1122.
22. Miyakawa, T., Mizushima, A., Hirose, K., Yamazawa, T., Bezprozvanny, I., Kurosaki, T., and Iino, M. (2001). Ca^{2+}-sensor region of IP_3 receptor controls intracellular Ca^{2+} signaling. EMBO J. *20*, 1674–1680.
23. Zacchetti, D., Clementi, E., Fasolato, C., Lorenzon, P., Zottini, M., Grohovaz, F., Fumagalli, G., Pozzan, T., and Meldolesi, J. (1991). Intracellular Ca^{2+} pools in PC12 cells. A unique, rapidly exchanging pool is sensitive to both inositol 1,4,5-trisphosphate and caffeine-ryanodine. J. Biol. Chem. *266*, 20152–20158.
24. Kim, Y.H., Park, T.J., Lee, Y.H., Baek, K.J., Suh, P.G., Ryu, S.H., and Kim, K.T. (1999). Phospholipase C-delta1 is activated by capacitative calcium entry that follows phospholipase C-beta activation upon bradykinin stimulation. J. Biol. Chem. *274*, 26127–26134.
25. Ogden, D., and Capiod, T. (1997). Regulation of Ca release by InsP3 in single guinea pig hepatocytes and rat Purkinje neurons. J. Gen. Physiol. *109*, 741–756.
26. Wilcox, R.A., Primrose, W.U., Nahorski, S.R., and Challiss, R.A.J. (1998). New developments in the molecular pharmacology of the *myo*-inositol 1,4,5-trisphosphate receptor. Trends Pharmacol. Sci. *19*, 467–475.
27. Rajfur, Z., Roy, P., Otey, C., Romer, L., and Jacobson, K. (2002). Dissecting the link between stress fibres and focal adhesions by CALI with EGFP fusion proteins. Nat. Cell Biol. *4*, 286–293.
28. Marek, K.W., and Davis, G.W. (2002). Transgenically encoded protein photoinactivation (FlAsH-FALI): acute inactivation of synaptotagmin I. Neuron *36*, 805–13.
29. Dilara, G., and Charles, W. (1999). Laser-mediated, site-specific inactivation of RNA transcripts. Proc. Natl. Acad. Sci. USA *96*, 6131–6136.